JPET #134551

Systemic Activation of the Transient Receptor Potential V4 Channel Causes Endothelial Failure and Circulatory Collapse: Part 2

Robert N. Willette, Weike Bao, Sandhya Nerurkar, Tian-li Yue, Chris P Doe, Gerald Stankus, Gregory H. Turner, Haisong Ju, Heath Thomas, Cindy E. Fishman, Anthony Sulpizio, David J. Behm, Sandra Hoffman, Zuojun Lin, Irina Lozinskaya, Linda N Casillas, Min Lin, Robert E. Lee Trout, Bartholomew J. Votta, Kevin Thorneloe, Erin S.R. Lashinger, David J. Figueroa, Robert Marquis, Xiaoping Xu

Cardiovascular-Urogenital (RNW, WB, SN, T-LY, CPD, GS, GHT, AS, DJB, IL, KT, ESRL, DJF, XX) and Oncology (SH, LNC, ML, RE LT, BJV, RM) Centers of Excellence in Drug Discovery, Safety Assessment (HJ, HT, CEF), GlaxoSmithKline Pharmaceuticals, King of Prussia, PA

JPET #134551

Running title: TRPV4 Mediates Endothelial Injury

Corresponding author:

Robert N. Willette, Ph.D.

Investigative & Cardiac Biology

GlaxoSmithKline Pharmaceuticals

709 Swedeland Road - UW2510

King of Prussia, PA 19406

telephone: 610-270-6052

fax: 610-270-5080

robert.n.willette@gsk.com

Pages : 24

Tables : 1

Figures : 8

References : 19

Abtract word count: 250

Introduction word count: 339

Discussion word count: 1190

List of non-standard Abbreviations:

AoSMC, human aortic smooth muscle cells

HAEC, human aortic endothelial cells

HUVEC, human umbilical vein endothelial cells

JPET #134551

PE, phenylephrine

RuR, ruthenium red

TRP, transient receptor potential

V4, vanilloid subtype 4

V1, vanilloid subtype 1.

Assignment: Cardiovascular Section

3

Abstract:

The transient receptor potential V4 (TRPV4) is a non-selective cation channel that exhibits polymodal activation and is expressed in endothelium where it contributes to intracellular Ca^{2+} homeostasis and regulation of cell volume. The purpose of the present study was to evaluate the systemic cardiovascular effects of GSK1016790A, a novel TRPV4 activator, and to examine its mechanism of action. In three species (mouse, rat and dog), the intravenous administration of GSK1016790A induced a dose-dependent reduction in blood pressure, followed by profound circulatory collapse. In contrast, GSK1016790A had no acute cardiovascular effects in the TRPV4$^{-/-}$ null mouse. Hemodynamic analysis in the dog and rat demonstrate a profound reduction in cardiac output. However, GSK1016790A had no effect on rate or contractility in the isolated, buffer-perfused rat heart and produced potent endothelial-dependent relaxation of rodent isolated vascular ring segments that was abolished by NOS inhibition (L-NAME), ruthenium red and eNOS gene deletion. However, the *in vivo* circulatory collapse was not altered by NOS inhibition (L-NAME) or eNOS gene deletion but was associated with (concentration and time appropriate) profound vascular leakage and tissue hemorrhage in the lung, intestine and kidney. TRPV4 immunoreactivity was localized in endothelium and epithelium in the affected organs. GSK1016790A potently induced rapid electrophysiological and morphological changes (retraction/condensation) in cultured endothelial cells. In summary, inappropriate activation of TRPV4 produces acute circulatory collapse associated with endothelial activation/injury and failure of the

pulmonary microvascular permeability barrier. It will be important to determine the role

of TRPV4 in disorders associated with edema and microvascular congestion.

JPET #134551

Introduction:

Evidence suggests that the transient receptor potential V4 (TRPV4), a member of the TRP family, is a thermo/osmo/mechanosensitive cationic channel that regulates intracellular Ca^{++}-homeostasis and cell volume (for review see Plant and Strotmann, 2007). The TRPV4 message is expressed in cardiovascular tissues (heart and blood vessels) and evidence of functional expression has been demonstrated in vascular smooth muscle and endothelial cells (Earley, 2006; Inoue, et al., 2006; Yang, et al., 2006). In the endothelium, activation of TRPV4 by ligands or shear-stress triggers NO-dependent vasorelaxation (Kohler et al., 2006). These studies suggest that TRPV4 activation is linked mechanistically to NO generation during the process of endothelial mechanotransduction.

TRPV4 also appears to play a role in fluid distribution and integrity of endothelial/epithelial barriers. Importantly, TRPV4 activation in the lung microvasculature increases endothelial and epithelial permeability and preferentially causes barrier disruption in alveolar septal regions (Alvarez, et al., 2006). Increased paracellular permeability associated with disruption of tight-junctions has also been associated with TRPV4 activation in the epithelium (Reiter, et al., 2006). Most recently, it has been demonstrated that TRPV4 is a major determinant of acute microvascular injury in the lung caused by mechanical ventilation and increased lung permeability induced by elevated pulmonary vascular pressure (Hamanaka et al., 2007; Jian et al., 2008). Taken together these results suggest that TRPV4 mechanisms impact local fluid distribution and modulate barrier integrity.

6

TRPV4 is expressed to some degree in vascular smooth muscle where activation by endogenous mediators (5,6-EET or 11,12-EET) or phorbol ester (4α-PDD) elicit a nifedipine-insensitive inward Ca^{++}-current (Yang, et al., 2006). In cerebral arteries TRPV4 activation is associated with Ca^{++}-mediated BK channel activation, hyperpolarization and vasodilation (Earley, 2006). However, this scenario is likely to be different in pulmonary vascular smooth muscle where 11,12-EET activates TRPV4 and is known to causes pulmonary vasoconstriction (Yang, et al., 2006).

Despite these compelling observations suggesting an important role of TRPV4 in cardiovascular homeostasis, there are no published reports describing the integrated circulatory actions of TRPV4 activation. The aims of the present study were to examine the systemic hemodynamic effects of a potent and selective TRPV4 agonist (GSK1016709A) and to probe the underlying functional mechanisms. Using standard isolated tissue and *in vivo* preparations we have found that TRPV4 activation produces dramatic and complex cardiovascular effects associated with endothelial barrier failure.

Materials and Methods:

All animal experiments were conducted in accordance with the Guide for the Care and use of Laboratory Animals (U.S. National Institutes of Health) and approved by the GlaxoSmithKline Animal Care and Use Committee.

In Vivo Hemodynamic Studies:

Hemodynamic measurement in anesthetized mice: Blood pressure and heart rate were evaluated in several mouse strains, i.e. wild type (TRPV4$^{+/+}$), TRPV4$^{+/-}$, TRPV4$^{-/-}$ (Charles River Laboratories;Wilmington, DE, USA), B6.129P2-NOS3/J (eNOS$^{-/-}$) and C57BL/6 (Jackson Laboratories; Bar Harbor, ME). Anesthesia was induced and maintained with isoflurane (1.5% in O_2). The right common carotid artery and jugular vein were isolated and cannulated with PE 50 cannulae for continuous monitoring of blood pressure, heart rate and for infusion of drugs. GSK1016790A doses were administered in an escalating fashion at the rate of 20ul/min in a total volume of 100ul. The vehicle was 1%DMSO/20% Captisol in saline.

Hemodynamic measurement in the anesthetized dog: Male Marshall Beagles weighing 8-12kg were fasted for 18 hours and were then anesthetized with Propofol® (10mg/kg i.v). A tracheotomy was performed and dogs were ventilated mechanically with room air. A Millar Microtip® transducer was placed into the left ventricle via the left carotid artery to monitor left ventricular pressure (LVP) and its first derivative (dP/dt).

A Swann-Gantz catheter was placed into the pulmonary artery via the right jugular vein. Position was verified by balloon inflation and demonstration of pulmonary wedge pressure. Femoral arteries and veins were isolated and an arterial catheter was inserted into the left femoral artery to monitor blood pressure. Catheters were inserted into femoral veins for drug and anesthesia administration. A left thoracotomy was performed at the third intercostal space and a 16mm Transonic® flow probe was placed around the ascending aorta to measure cardiac output. Blood gas measurements were routinely performed and maintained within normal limits until administration of GSK1016790A. Anesthesia was maintained with alpha chloralose (65mg/kg i.v.+ 0.5mg/kg/min). All parameters were continuously recorded on CA Recorder computer software. Dogs were allowed to equilibrate for 30-60 minutes prior to drug administration. GSK1016790A was administered as an ascending intravenous infusion and each dose, beginning with vehicle, was infused for 15 minutes. Some dogs were administered the autonomic ganglia blocker hexamethonium chloride (5mg/kg i.v. followed by a 100 ug/kg/min infusion) prior to administration of GSK1016790A. The vasopressor response induced by temporarily occluding the right common carotid artery recorded before and after hexamethonium chloride administration to verify ganglionic blockade.

Evans Blue Distribution, Histology and TRPV4 Immunohistochemisty:

Vascular permeability was assessed grossly as described previously (Sulpizio, et al., 2005),   Briefly, rats and mice were anesthetized as described above, and catheters were placed in the carotid artery and jugular vein for the direct measurement of blood pressure and drug administration, respectively. After a 10 min equilibrium period,

animals received an intravenous bolus (2ml/kg) of Evans blue dye (15 mg/ml, containing heparin 33 units/ml) followed by infusion of GSK1016790A (30 ug/ml @ 0.1 ml/min). In the low dose group the infusion of GSK1016790A was discontinued when the BP was reduced 20 mmHg. In the high dose group, the infusion was terminated when the BP was reduced > 50 mmHg. The approximate dose in the low and high dose groups were 30 ug/kg and 60 ug/kg, respectively. Immediately following drug infusion the thoracic cavity was opened by single midline incision, the animal was exsanguinated by cutting open the right atrium and the left ventricle was perfused with normal saline at 100 mmHg until the perfusate was clear. The tissue distribution of Evans Blue was assessed grossly and photographed during the postmortem examination. Evans blue dye was purchased from Sigma-Aldrich (Saint Louis, MO, USA).

Histologic assessment of tissues was performed in 4 groups of rats (n=3-4 per group). One group received a vehicle infusion and three received GSK1016790A (30 ug/ml @ 0.1 ml/min). GSK1016790A groups were dosed to effect, i.e. decrease BP by 20 mmHg, 50 mmHg and $\geq$ 70 mmHg (circulatory collapse). Organs were rapidly removed, sliced and immersed in 10% buffered formalin overnight. Histologic sections prepared from the liver, kidney, aorta, heart, lung, colon, cecum, small intestine, and mesentery were examined independently by board certified veterinary pathologists (HT & CF). The tissues were embedded in paraffin wax and sectioned at 5 μm followed by hematoxylin and eosin staining.

Immunohistochemistry:

Twelve week old Sprague-Dawley rats (Charles River Labs) were euthanized, and heart, liver, brain, small intestine, kidney and lung tissues were fixed by immersion in 4% paraformaldehyde (Electron Microscopy Sciences) and processed to paraffin. A polyclonal antibody specific for a synthetic peptide identical to the first sixteen amino acids of rat TRPV4, MADPGDGPRAAPGDVA, was prepared in rabbits and affinity purified (Invitrogen). Eight micron thick paraffin sections were de-waxed and subjected to antigen retrieval. Antigen retrieval was performed by a steam heat method with Citra Solution buffer (Biogenex) at 95°C for 15 minutes. The sections were sequentially blocked for endogenous biotin binding using the Vector blocking kit (Vector Laboratories), endogenous peroxidase activity with a 1% hydrogen peroxide, 0.2 M sodium azide solution in PBS, and then with 10% normal goat serum (Jackson Immunoresearch) in staining buffer. The TRPV4 specific antibody was incubated on the sections at a concentration of 2.0 ug/ml overnight at room temperature. A purified rabbit IgG (Zymed Laboratories, Invitrogen) was used at the same concentration as a negative control. Bound TRPV4 antibody was detected by the standard avidin-biotin indirect peroxidase immunohistochemical technique using a biotinylated rabbit anti-rat IgG (Vector Laboratories) in combination with the Vector Elite ABC system (Vector Laboratories). Staining was visualized with 3,3′-diaminobenzidine tetrahydrochloride (DAB) substrate (DAKO) and the sections were then counterstained with Harris' hematoxylin (Thermo Shandon Lipshaw, Pittsburg, PA). Images were acquired using a Nikon E80i microscope (Nikon, Tokyo, Japan), a Nikon DXM 1200C camera (Optical Apparatus Inc,) and Nikon Elements BR imaging program (Nikon, Tokyo, Japan).

In Vitro Vascular and Cardiac Studies:

Mouse and Rat Aortic ring segments: Vascular reactivity studies were performed

as described previously (Behm, et al., 2003). Male eNOS knock-out mice (and

corresponding wild-type littermates) and female Sprague Dawley rats were euthanized

via cervical dislocation (while anesthetized with 5% isoflurane in O_2) or CO_2

asphyxiation, respectively. The thoracic aorta was isolated, cleaned of adherent tissue

and cut into 3mm rings. Each ring was suspended in organ baths containing Krebs of the

following composition (mM): NaCl, 112.0; KCl, 4.7; KH_2PO_4, 1.2; $MgSO_4$, 1.2; $CaCl_2$,

2.5; $NaHCO_3$, 25.0; dextrose, 11.0. Krebs was maintained at 37ºC and aerated with

95%O_2:5%CO_2 (pH 7.4). Standard force displacement transducers and recording

apparatus (MLT0201/D; Letica Scientific Instruments, ADInstruments, TSD125,

BIOPAC Systems, Inc.) were used to measure changes in aortic isometric force. Resting

tension for vascular ring segments in the mouse was set to 0.5 g and 1.0 g in the rat. In

some rat aortic segments the endothelium was removed by passing an 18 gauge 1.5 inch

hypodermic needle through the lumen of the ring and gently rubbing the interior of the

vessel against the needle shaft. Once mounted in the tissue bath the arteries were allowed

to equilibrate for 45-60min and viability was assessed by recording and washing out

responses to 60mM KCl and 100 nM phenylephrine . The functional integrity of the

aortic endothelium was determined by evaluation of carbachol-induced (10μM mouse;

1μM rat) relaxation in vessels precontracted with phenylephrine (100 nM). Following

washout, tissues were again pre-contracted with an EC_{80} concentration of phenylephrine

(100 nM) and single point or concentration-response experiments were performed to assess GSK1016790A-induced vasorelaxation. DMSO (10 ul) was used as a vehicle/time control. Some endothelium intact rat aorta segments were pretreated for 30min with L-NAME ($100\mu M$) prior to contraction with phenylephrine. All responses were allowed to reach steady-state prior to changes in concentration. Data are expressed as the mean % change in the phenylephrine-induced contraction ± SEM.

Langendorff perfused heart: As described previously (Yue, et al., 2000), male Sprague-Dawley rats (~350 g) were anesthetized with intraperitoneal injection of Nembutal 60/kg and heparinized with sodium heparine 200 IU/kg. The hearts were rapidly excised and transferred in ice-cold buffered Krebs-Henseleit solution, consisting of 118.5 mM NaCl, 4.7 mM KCl, 1.2 mM $CaCl_2$, 1.2 mM $MgSO_4$, 25 mM $NaHCO_3$, 1.2 mM KH_2PO_4, 11 mM glucose, bubbled with 95% O_2, 5% CO_2; pH 7.4. A retrograde aortic cannula was immediately placed and connected to the Langendorff apparatus (ISOLATED HEART Size 1 (IH-1), Harvard apparatus, USA) to start buffer perfusion at a constant pressure of 70 mmHg ($37^{o}C$). A water-filled latex balloon, connected to a blood pressure transducer, was inserted through the mitral valve into the left ventricle. The balloon was inflated with water until the left ventricular end diastolic pressure was 5-8 mmHg and isovolumic left ventricular developed pressures were recorded to a digital data acquisition system. Vehicle and drug were added to the perfusion buffer.

Cell cultures and morphological assessment: Human umbilical vein endothelial cells (HUVEC) and human aortic smooth muscle cells (AoSMCs) were obtained from

Lonza (Walkersville, MD). HUVEC were grown in endothelial basal medium supplemented with growth factors and 2% fetal bovine serum (Lonza) and AoSMCs were grown in Dulbecco's modified eagle's medium (DMEM) supplemented with 10% fetal bovine serum in a humidified environment of 5% CO_2, 95% air at 37^0C. Cells were grown in 2-well chamber slides (Lab-Tek) and used at a sub-confluent density. Before experiments, the medium was changed to basal medium containing 2% fetal bovine serum for HUVECs and AoSMCs.

Cells treated with vehicle or GSK1016790A for the indicated time intervals were gently washed with PBS, and fixed with 4% paraformaldehyde, and stained with Giemsa stain (Sigma). For cell imaging, HUVECs were fixed, permeabilized, and stained with mouse anti- human α-tubulin antibody (1:100), followed by goat anti mouse IgG conjugated with Alexa Fluro 488 (1:500) (Invitrogen, Carlsbad, CA).

To quantify the cells attachment after GSK1016790A treatment, ten randomly selected fields from each slide were counted double blinded. Cell counts from the vehicle treatment were normalized as 100%.

Patch-clamp Analysis:

Human aortic endothelial cells (HAECs) were purchased from Lonza Bioscience (Catalogue #CC-2535) and cultured according to the suppliers instructions. Whole-cell patch-clamp experiments were performed on HAECs at passage 5. Experimental conditions were similar to what have been described previously (Zeng, et al., 2006)(Zeng, et al., 2006). Patch-clamp pipette solution (in mM): 140 KCl, 5 EGTA, 1 $MgCl_2$, 5 MgATP, 0.2 $CaCl_2$, 5 HEPES; pH = 7.2. External solution (in mM): 140 NaCl, 4 KCl, 1

$MgCl_2$, 2 $CaCl_2$, 10 Glucose, 10 HEPES; pH = 7.4. The membrane current was elicited in

HAECs using a ramp voltage-clamp protocol repeated every 10-s (holding potential = -80

mV, depolarizing from -100 mV to +80 mV in 700-ms) at room temperature.

Drugs and formulations:

The TRPV4 agonist, GSK1016790A, shown in Figure 1 was synthesized in the

Department of Medicinal Chemistry of the Oncology Center of Excellence in Drug

Discovery, GlaxoSmithKline as detailed in patent application WO 2007070865 (Casillas

and Marquis, 2007) for the purpose of investigating the biology of the TRPV4 channel in

a variety of systems. GSK1016790A for in vivo administration was prepared in a vehicle

of 1%DMSO/20% Captisol in saline and in DMSO (0.1%) for in vitro studies.

Statistical Analysis:

Data are presented as mean ± SEM. Differences between groups were compared

by paired and unpaired Student's t tests or by ANOVA followed by a Bonferroni test. P

values of < 0.05 were considered statistically significant.

Results:

Characterization of GSK1016790A, a TRPV4 activator:

GSK1016790A is a recently described novel chemical entity that potently activates TRPV4 channels in a variety of recombinant and native cellular assays (Figure 1A). GSK1016790A has single digit nM potency in human, dog and bovine cellular assays (1.0 -5.0 nM) and is slightly less potent in rodent assays (10-18.5 nM). Selectivity is approximately 10-fold with regard to the highly homologous TRPV1 cation channel. The addition of GSK1016970A (10 nM) to the recording chamber (exterior of the cell) activated both inward and outward current in HAECs (Fig. 1B). The activated current showed some outward rectification and had a reversal potential near 0 mV. The GSK1016970 activated current was largely inhibited by RuR (5 μM), a non-specific TRP channel blocker. GSK1016790A had approximately 1000-fold greater potency than the standard TRPV4 activator, 4α-DPP (data not shown).

Hemodynamic studies:

In wild type mice (TRPV$^{+/+}$), the intravenous administration of GSK1016790A induced a dose-dependent reduction in blood pressure that culminates in cardiovascular collapse at the highest dose (Fig. 2A). The threshold dose was approximately 0.03 mg/kg (data not shown), the depressor dose was 0.1 mg/kg, and the lethal dose was 0.3 mg/kg (n=3). The TRPV4$^{+/-}$ heterozygotic strain exhibited reduced sensitivity to the blood pressure effects of GSK1016790A (Fig. 2B) – the depessor dose was 0.3 mg/kg and the

lethal dose was 1.0 mg/kg (n=3). TRPV4 gene deletion (TRPV4$^{-/-}$) abolished the

hemodynamic effects of GSK1016790A (Fig. 2C). Vehicle administration had no

significant effect on BP (as in Fig. 2C).

GSK1016790A was examined in greater detail in the anesthetized dog to

determine the hemodynamic events responsible for TRPV4 -mediated circulatory

collapse. Similar to the mouse, the intravenous administration of GSK1016790A caused

a reduction in blood pressure and eventual circulatory failure in the dog. At the threshold

dose (0.3 μg/kg/min), modest reductions in mean arterial pressure (MAP) and systemic

vascular resistance (SVR) were observed (Fig 3). The circulatory collapse observed at

1.0 μg/kg/min was clearly related to acute cardiac output failure determined largely by a

reduction in stroke volume. Pretreatment with the ganglionic blocker, hexamethonium,

did not alter the overall pattern of the hemodynamic response, however the magnitude of

the collapse was exaggerated. GSK1016790A had similar hemodynamic effects in the rat

(see Fig. 5).

Isolated perfused rat heart:

In order to investigate the direct cardiac effects of TRPV4 activation,

GSK1016790A was examined in isolated buffer-perfused rat hearts where left ventricular

function was monitored by recording developed pressure in a balloon tipped catheter

inserted in the left ventricle. GSK1016790A (1.5-13.5 μM) in the perfusate had no effect

on spontaneous rate or contractility in the isolated-perfused rat heart (Table 1).

JPET #134551

Vascular reactivity and role of eNOS in circulatory collapse:

Direct vascular effects of GSK1016790A were investigated in rat and mouse by recording isometric tension from isolated aortic ring segments suspended in organ baths containing Krebs-Henseleit buffer. The addition of GSK1016790A to the organ bath had no effect on resting tension in any of the preparations (data not shown) but caused potent and efficacious relaxation of vessels pre-contracted with phenylephrine (Fig. 4A&B). In Fig. 4A, maximal relaxation induced by GSK1016790A was abolished by endothelial denudation, NOS inhibition (L-NAME), and the TRP channel blocker RuR. Similarly, GSK1016790A-induced relaxation of the thoracic aorta was not observed in mice lacking eNOS (Fig 4B). However, circulatory collapse induced by GSK1016790A (n=3) was unaltered in the $eNOS^{-/-}$ strain (Fig. 4C).

Vascular permeability:

Cardiac MRI and the tissue distribution of Evan's Blue were examined grossly in rats following the administration of GSK1016790A at vasodepressor doses and lethal doses. At the lethal dose, cardiac MRI (Fig. 5A) indicate signs of acute right ventricular failure characterized by right ventricular dilation with septal shift (Fig. 5B) that was accompanied by elevated pulmonary arterial pressure (Fig. 5C). GSK1016790A elicited dose-dependent extravasation of Evan's Blue and/or obvious vascular hemorrhage, within minutes of administration in the lung (Fig. 5D&E), large intestine and kidney (data not shown) at the nadir of the blood pressure response. At 15 minutes following GSK1016790A (0.3 mg/kg/15 min) the lung wet weight to body weight (LW:BW) ratio was increased approximately 2.5-fold when compared to vehicle (0.2 ml 1% DMSO,

18

29% β-cyclodextrin. The profound effects of GSK101670A in the lung were associated with histologic changes that included evidence of pulmonary edema and congestion associated with perivascular hemorrhage and multifocal alveolar hemorrhage Fig. 5G & H). At a dose (30-100 ug/kg, iv) causing a 20 mmHg reduction in blood pressure there were no drug-related abnormalities detected, i.e. similar to vehicle infused animals (data not shown). Significant histologic changes were also observed in the large intestine and included dose-dependent submucosal and mucosal edema ranging in severity from minimal to moderate (depicted in supplemental Fig. 1). In the kidney, there was a dose-dependent acute medullary tubular necrosis which ranged in severity from minimal to moderate. Additionally, there was evidence of tubular and peritubular hemorrhage. It is notable that Evan's blue extravasation and hemorrhage were not observed grossly in brain, heart, liver, pancreas or skeletal muscle, and there was no evidence of hemorrhage in the other tissues examined histologically. Similar results were observed in wild type mice but not in the TRPV4$^{-/-}$ strain.

Immunohistochemical localization of TRPV4:

Immunohistochemical localization of TRPV4 was examined in a variety of rat tissues to investigate expression patterns that may underlie the heterogeneous effects of GSK101670A on microvascular permeability. A generalized pattern of immunoreactive TRPV4 staining was identified in endothelium and epithelium. In the lung, robust TRPV4 staining was observed in epithelium lining secondary and tertiary segments of the airway and in endothelium of bronchial and pulmonary artery endothelium (Fig. 6A&C). Large arteries also exhibited a more variable pattern of TRPV4 staining in the

adventitium. A lacey pattern of TPV4 staining was also evident in alveolar septal regions. Vascular and bronchial smooth muscle were devoid of TRPV4 immunoreactivity.

In the kidney, TRPV4 immunoreactive staining patterns were morphologically consistent with a previous description (Tian, et al., 2004) i.e robust TRPV4 staining in the nephron epithelium included ascending thick limb, distal convoluted tubule, ascending thin limb and inner medullary collecting duct (Fig. 6F&G). The renal arcuate artery endothelium was consistently positive for TRPV4 immunoreactivity. Arterial smooth muscle, proximal tubular segments and glomeruli were negative. A similar general pattern of endothelial and epithelial TRPV4 immunoreactivity without smooth muscle staining was observed in the small intestine (Fig. 6 D&E).

Blood vessels throughout the brain and heart also exhibited highly restricted endothelial TRPV4 immunoreactivity (Fig. 7A,B&D). With the exception of the choroid in cerebral ventricles (Fig. 7C), which was strongly positive (as described by Liedtke et al., 2000), there was little or no extravascular TRPV4 immunoreactivity in the heart and only highly restricted circumventricular staining in the brain (not shown).

Endothelial and Vascular Smooth Muscle Cell Culture:

The cellular events underlying microvascular damage induced by TRPV4 activation were investigated in cultures of human umbilical vein endothelial cells (HUVEC) and human aortic smooth muscle cells (AoSMC). The addition of GSK1016790A to culture media caused a potent (10 nM) and rapid (within 10 min) retraction and condensation of HUVEC (Fig. 8A&B). More prolonged incubation (30 mins) with GSK1016790A caused a concentration-related detachment of HUVEC from

JPET #134551

the plate (Fig. 8G&H).   The effects GSK1016790A on HUVEC were abolished by

pretreatment with the TRP channel blocker RuR (Fig. 8C&D).   In contrast to the

HUVEC, GSK1016790A (100 nM) had no effect on morphology or adhesion in AoSMC

(Fig.8 E&F) or human small airway epithelial cell cultures (data not shown).   The results

suggest that failure of the endothelial permeability barrier induced by TRPV4 activation

is mediated by direct effects on endothelial cell morphology.

Discussion:

In the present study we characterized a novel synthetic TRPV4 channel activator, GSK1016790A, and examined its cardiovascular effects. We provide evidence supporting the role of TRPV4 in Ca^{++}-dependent regulation of endothelial NO production and describe for the first time catastrophic cardiovascular effects associated with exogenous activation of TRPV4. Moreover, we provide evidence that circulatory collapse induced by TRPV4 activation is mediated by an NO-independent failure of the endothelial-epithelial permeability barrier in the lung and other selected tissues.

GSK1016790A is a novel and potent small molecule activator of the TRPV4 channel (Casillas and Marquis, 2007). It is structurally unrelated to phorbol ester TRPV4 activators and possesses relative selectivity with regard to highly homologus TRPV1 channels (devoid of cardiovascular effects). In addition, GSK1016790A retains nM potency at its target across a variety of species making it an attractive tool for investigating the pharmacology and physiology of TRPV4 channels.

In vivo, the intravenous administration of GSK1016790A induced a dose-related depression of blood pressure followed by circulatory collapse in wild type (WT) mice, rats and dogs. In contrast, GSK1016790A had no effect on BP or HR in TRPV4^{-/-} null mice at doses >10-fold the lethal dose in WT mice and, heterozygous TRPV4^{+/-} mice were slightly more resistant to the lethal effects of GSK1016790A (approximately 3-fold the lethal dose in WT). These results clearly demonstrate the role of TRPV4 in mediating the cardiovascular effects of GSK1016790A. It is noteworthy that TRPV4 deficient mice were normotensive (data not shown). Hemodynamic analysis of GSK1016790A in

mechanically ventilated anesthetized dogs was characterized by a reduction in cardiac output associated primarily with decreased stroke volume and delayed bradycardia. In order to eliminate reflex adjustments and focus on the primary actions of GSK1016790A, hemodynamic effects were examined in dogs following autonomic blockade with hexamethonium. Under these conditions, the hemodynamic actions of GSK1016790A were qualitatively similar, albeit greater in magnitude, when compared to the intact preparation, i.e. a slight decrease in systemic vascular resistance associated with a moderate reduction in BP that was rapidly followed by the cardiac failure described above. These *in vivo* results suggest that GSK1016790A severely depressed cardiac function and only modestly reduced vascular tone.

Evidence suggests that the vascular effects of TRPV4 activation are, in some instances, mediated by endothelial NO generation (Kohler, et al., 2006). As such, we evaluated the effects of pharmacologic and genetic manipulation of eNOS on the vascular and hemodynamic effects of GSK1016790A. In preconstricted mouse and rat isolated aortae, GSK1016790A induced potent and efficacious relaxation. The actions of GSK1016709A in the aorta were absent in vessels obtained from TRPV4 null mouse and abolished by the non-selective TRP channel blocker, ruthenium red. These results suggest that the vascular relaxation induced by GSK1016790A was mediated specifically by activation of the TRPV4 channel. Furthermore, aortic relaxation induced by GSK1016790A was absent in eNOS null mice and abolished by endothelial denudation and inhibition of nitric oxide synthase (L-NAME). The present results are consistent with previously described expression of TRPV4 in endothelial cells (Yao and Garland, 2005;Kwan HY, 2007) and with a recent report describing endothelial/NO-dependent

relaxation of isolated rat carotid artery with a selective TRPV4 activator, 4α-phorbol-12,13-didecanoate (Kohler, et al., 2006). Taken together, the results suggest that potent exogenous activation of TRPV4 is a powerful endothelial-dependent mechanism, regulating vascular tone via eNOS activation and NO generation.

Hemodynamic mechanisms of GSK1016790A were further examined *in vivo* in eNOS null mice and L-NAME treated rats. Somewhat surprisingly the hemodyanmic effects and lethal dose of GSK1016790A were indistinguishable in eNOS null and WT mice. Similarly, L-NAME treatment failed to alter the circulatory collapse in rats. Thus the TRPV4-mediated endothelial NO generation, which played a critical role in GSK1016790A-induced vasorelaxation, appears to play little or no role in TRPV4-mediated circulatory failure.

In addition, GSK1016790A had no effects on inotropy or chronotropy in the isolated rat heart. Again the results were surprising given the profound *in vivo* effects of GSK1016790A on cardiac output; however, the lack of effect is consistent with the paucity of TRPV4 expression in cardiomyocytes demonstrated by TRPV4 immunohistochemistry.

Recent evidence suggests that TRPV4 activation, whether by exogenous activators or by elevated vascular and/or inspiratory pressure, induces a heterogeneous increase in pulmonary endothelial permeability (Alvarez, et al., 2006; Hamanaka et al., 2007). In the present study GSK1016790A caused a dose-dependent increase in microvascular permeability (Evans Blue leakage) and hemorrhage in the lung, kidney and intestine. The microvascular injury in the lung was associated with histological changes that included pulmonary edema and congestion associated with perivascular hemorrhage

and multifocal alveolar hemorrhage and was related to the magnitude of the

hemodynamic response. The lung injury was associated with pulmonary hypertension

and right heart failure that most likely obscure observation of NO-related hemodynamic

effects. It is noteworthy that in the present study evidence of gross microvascular injury

was not apparent in heart, brain, liver or skeletal muscle suggesting a heterogeneous

microvascular response to TRPV4 activation.

The present results provide evidence for localization and function of TRPV4

channels in vascular endothelium that is consistent with a role in the regulation of

vascular permeability. However, the data do not provide a clear explanation for the organ

specific changes in vascular permeability observed following TRPV4 activation *in vivo*.

A paucity of TRPV4 channels in resistant organs, e.g. heart and brain, can not be strictly

ruled out, but it seems highly unlikely given the robust endothelial TRPV4

immunoreactivity in these organs. One commonality in the sensitive organs (lung,

intestine and kidney) is the unique juxtaposition of TRPV4 positive epithelium and

endothelium. Thus, it is tempting to speculate that *in vivo* activation of TRPV4 in both of

these cell types plays a cooperative role in mediating the effects of GSK1016790A on

vascular permeability. Temporal considerations and cell specific TRPV4 signaling are

also areas for future study.

At the cellular level, GSK1016790A caused apparent cytoskeletal reorganization

characterized by rapid endothelial cell retraction/contraction, condensation and

subsequent detachment. All morphologic changes in endothelial cells were inhibited by

ruthenium red. These results are consistent with the complex interactions of eNOS, TRPs

and the cytoskeleton that are known to exist at endothelial caveoli microdomains and are

analogous to actions attributed to TRPC4 (Govers and Rabelink, 2001;Tiruppathi, et al., 2006).   In contrast to endothelial cells, the morphology of vascular smooth muscle cells and small airway epithelial cells (data not shown) was not affected by GSK1016790A. In addition, GSK1016790A did not contract isolated rat pulmonary artery (data not shown). The results suggest that TRPV4 activation causes disruption of the microvascular permeability barrier by directly altering endothelial morphology and integrity.

In conclusion, a novel TRPV4 activator was used to describe, for the first time, TRPV4-dependent circulatory collapse. Failure of the cardiac output was not related to TRPV4-dependent endothelial NO generation or direct myocardial actions. Evidence suggests that the circulatory collapse is the result of profound disruption of the endothelial permeability barrier in the lung and attendant acute pulmonary hypertension and right heart failure. Given the powerful effects of TRPV4 on microvascular integrity, it will be important to further define its role in endothelial function and vascular disease.

JPET #134551

References:

Alvarez DF, King JA, Weber D, Addison E, Liedtke W and Townsley MI (2006)
Transient receptor potential vanilloid 4-mediated disruption of the alveolar septal barrier.
Circulation Research 99:988-995.

Behm DJ, Harrison SM, Ao ZH, Maniscalco K, Pickering SJ, Grau EV, Woods TN,
Coatney RW, Doe CPA, Willette RN, Johns DG and Douglas SA (2003) Deletion of the
UT receptor gene results in the selective loss of urotensin-II contractile activity in aortae
isolated from UT receptor knockout mice. *British Journal of Pharmacology* 139:464-472.

Casillas LN and Marquis RW.   Preparation of piperazine-containing peptidomimetics
for use in treatment of diseases associated with TRPV4 channel receptor.   PCT
Int.Appl.(2007) *WO 2007070865* A2 20070621 CAN 147:95915 AN 2007:670670 ,
85pp. 2007.

Earley S (2006) Molecular diversity of receptor operated channels in vascular smooth
muscle - A role for heteromultimeric TRP channels? *Circulation Research* 98:1462-1464.

Govers R and Rabelink TJ (2001) Cellular regulation of endothelial nitric oxide synthase
[Review]. *American Journal of Physiology - Renal Physiology* 280:F193-F206.

Hamanaka K, Jian M-Y, Weber D, Alvarez DF, Townsley MI, Al-Medi AB, King JA,
Liedtke W, Parker JC. (2007) TRPV4 inititates the acute calcium-dependent permeability
increases during ventilator-induced lung injury in isolated mouse lungs.. American
Journal of Physiology - Lung Cellular & Molecular Physiology 293: L923-L932.

JPET #134551

Inoue R, Jensen LJ, Shi J, Morita H, Nishida M, Honda A and Ito Y (2006) Transient receptor potential channels in cardiovascular function and disease [Review]. *Circulation Research* 99:119-131.

Jian M-Y, King, JA Al-Mehdi A-B Liedtke W and Townsley, M. (2008) High Vascular Pressure-induced Lung Injury Requires P450 Epoxygenase-dependent Activation of TRPV4 Am.J.Respir.Cell Mol.Biol. 38:386-392.

Kohler R, Heyken WT, Heinau P, Schubert R, Si H, Kacik M, Busch C, Grgic I, Maier T and Hoyer J (2006) Evidence for a functional role of endothelial transient receptor potential V4 in shear stress-induced vasodilatation. *Arteriosclerosis, Thrombosis & Vascular Biology* 26:1495-1502.

Kwan HY, Huang Y and Yao XQ (2007) TRP channels in endothelial function and dysfunction [Review]. *Biochimica et Biophysica Acta - Molecular Basis of Disease* 1772:907-914.

Liedtke W, Choe Y, Marti-Renom MA, Bell AM, Denis CS, Sali A, Hudspeth AJ, Friedman JM and Heller S (2000) Vanilloid receptor-related osmotically activated channel (VR-OAC), a candidate vertebrate osmoreceptor. *Cell* 103:525-535.

Plant TD and Strotmann R. TRPV4. Handbook of Experimental Pharmacology 179, 189-205. 2007.

Reiter B, Kraft R, Gunzel D, Zeissig S, Schulzke JD, Fromm M and Harteneck C (2006) TRPV4-mediated regulation of epithelial permeability. *FASEB Journal* 20:1802-1812.

Sulpizio AC, Pullen MA, Edwards RM, Louttit JB, West R and Brooks DP (2005) Mechanism of vasopeptidase inhibitor-induced plasma extravasation: Comparison of omapatrilat and the novel neutral endopeptidase 24.11/angiotensin-converting enzyme inhibitor GW796406. *Journal of Pharmacology & Experimental Therapeutics* 315:1306-1313.

Tian W, Salanova M, Xu HS, Lindsley JN, Oyama TT, Anderson S, Bachmann S and Cohen DM (2004) Renal expression of osmotically responsive cation channel TRPV4 is restricted to water-impermeant nephron segments. *American Journal of Physiology - Renal Physiology* **287**:F17-F24.

Tiruppathi C, Ahmmed GU, Vogel SM and Malik AB (2006) Ca2+ signaling, TRP channels, and endothelial permeability. *Microcirculation* **13**:693-708.

Yang XR, Lin MJ, McIntosh LS and Sham JSK (2006) Functional expression of transient receptor potential melastatin- and vanilloid-related channels in pulmonary arterial and aortic smooth muscle. *American Journal of Physiology - Lung Cellular & Molecular Physiology* **290**:L1267-L1276.

Yao XQ and Garland CJ (2005) Recent developments in vascular endothelial cell transient receptor potential channels [Review]. *Circulation Research* **97**:853-863.

Yue TL, Wang CL, Gu JL, Ma XL, Kumar S, Lee JC, Feuerstein GZ, Thomas H, Maleeff B and Ohlstein EH (2000) Inhibition of extracellular signal-regulated kinase enhances ischemia/reoxygenation-induced apoptosis in cultured cardiac myocytes and exaggerates reperfusion injury in isolated perfused heart. *Circulation Research* **86**:692-699.

JPET #134551

Zeng HY, Lozinskaya IM, Lin ZJ, Willette RN, Brooks DP and Xu XP (2006)

Mallotoxin is a novel human Ether-a-go-go-related gene (hERG) potassium channel

activator. *Journal of Pharmacology & Experimental Therapeutics* **319**:957-962.

Robert N. Willette, Ph.D.

Investigative & Cardiac Biology

GlaxoSmithKline Pharmaceuticals

709 Swedeland Road - UW2510

King of Prussia, PA 19406

telephone: 610-270-6052

fax: 610-270-5080

robert.n.willette@gsk.com

JPET #134551

Legends for Figures:

Figure 1: The chemical structure and *in vitro* characterization of GSK1016790A in recombinant cellular assays and across species in native cells (A). GSK1016790A activates a cationic current in primary cultured human aorta endothelial cells (B). Top: time course of the membrane current measured at +80 mV and -95 mV. Horizontal bars indicate external drug application. Bottom: current/voltage relationship in control, 10 nM GSK1016790A and 10 nM GSK1016790A in the presence of 5 µM ruthenium red (RuR).

Figure 2: Typical tracings illustrate the effects of GSK1016790A on mean arterial pressure (MAP) in wild type (TRPV4$^{+/+}$) and congenic mouse strains (TRPV4$^{+/-}$, TRPV4$^{-/-}$, eNOS$^{-/-}$). Vasodeperession and circulatory collapse were observed in all strains except TRPV4$^{-/-}$ (D). All doses (mg/kg) were administered at arrows in a volume of 100µl (20µl/min).

Figure 3: The effect of 15 min intravenous infusions of vehicle (V) or GSK1016790A (0.1, 0.3 and 1.0 ug/kg/min) on mean arterial pressure (MAP; panel A), heart rate (HR; panel B), cardiac output (CO; C) and systemic vascular resistance (SVR; panel D) in the presence or absence of ganglion blocking doses of hexamethonium (Hex) in chloralose anesthetized dogs (n=4/ group).

Figure 4: Relaxation induced by GSK1016790A in rat aortic rings from endothelium intact, endothelium denuded and L-NAME (100 µM) treated groups (A) and in aortic

32

rings prepared from wild type and eNOS null mice (B). Rat and mouse preparations were precontracted with phenylephrine (100 nM). Typical tracing of the mean arterial blood pressure effect of GSK1016790A in eNOS null mice (C, n=3). The values in A and B are mean ± SE, *$p<0.01$ vs. GSK1016790A, (n=4-8/group).

Figure 5: Representative results of the TRPV4 activator, GSK1016790A, in the anesthetized Sprague-Dawley rat. End-diastolic cardiac MRI following intravenous vehicle infusion at 0.1 ml/min (A) or infusion of GSK1016790A over a dose-range (50-113 ug/kg, iv) sufficient to induce circulatory collapse (B). Panel C illustrates changes in pulmonary arterial pressure observed following the infusion of GSK1016790A (arrow). Evan's blue extravasation in the lung following vehicle (D), or GSK1016790A administration sufficient to cause circulatory collapse (E). In panel F, the lung weight to body weight ratio (LW:BW) was determine 15 mins after the administration of vehicle (1% DMSO + 29% beta cyclodextrin) or GSK1016790A (0.3 mg/kg/min). Representative pulmonary histological findings are illustrated in panels G and H following the administration of vehicle and GSK1016790A, respectively (H). All observations represent of 3-5 replicates.

Figure 6: Immunohistochemical localization of TRPV4 in normal rat lung (A-C), small

intestine (D&E) and kidney (F&G); immunoperoxidase staining with hematoxylin

counterstaining. TRPV4-positive structures (brown) were morphologically consistent

epithelium and endothelium in respective organs.   Panel B is a preimmune rabbit IgG

negative control. Abbreviations: ASR, alveolar septal region; ATL, ascending thin limb;

Br, bronchiole; CT, convoluted tubule; EC, endothelium; PA, pulmonary artery; PAr,

pulmonary arteriole; SBV, submucosal blood vessel; SM, submucosal smooth muscle;

VSM, vascular smooth muscle. All scale bars equal 15 uM.

Figure 7: Immunohistochemical localization of TRPV4 in normal rat heart (A&B) and

brain (C&D) immunoperoxidase staining with hematoxylin counterstaining. TRPV4-

positive structures (brown) were morphologically consistent epithelium and endothelium

in respective organs.   Abbreviations: CM, cardiac muscle; CAE, cerebral arteriole

endothelium; ECP, epithelium of the choroid plexus; ICA, intramural coronary arterioles;

VSM, vascular smooth muscle. All scale bars equal 15 uM.

Figure 8: Effect of TRPV4 activator GSK1016790A on human umbilical vein

endothelial cells (HUVEC, panels A-D) and human aortic smooth muscle cells (AoSMC,

panels E&F). Cells were treated with vehicle (0.1% DMSO) (A & E), GSK1016790A (B

& F), ruthenium red alone (RuR) (C), or RR with GSK1016790A (D) at the

concentrations indicated. The inserts in A and B were HUVEC stained with anti-α-

tubulin.   Rightward panels depict the time (H) and concentration (G) -dependent effects

of GSK1016790A on HUVEC attachment to the plate in the absence or presence of 1 µM

ruthenium red (RuR). HUVEC were preincubated with RuR for 20 minute prior to the

addition of GSK1016790A (10 nM) for 3 hours (H). The values are mean ± SE.

**$p<0.001$ vs. the vehicle.

JPET #134551

Table 1. The Effect of GSK1016790A in the Isolated Perfused Rat Heart

GSK1016790A (µM)	HR (%)	LVDP (%)	dP/dt_{ma} (%)	dP/dt_{mi} (%)
0	99±3.9	103±1.7	104±0.6	104±0.0
1.5	97±2.3	106±3.8	107±3.8	108±5.8
4.5	92±11	103±6.5	101±10	95±2.9
13.5	99±4.0	99±1.2	98±2.8	98±6.8

All values are expressed as mean percent change in baseline. Abbreviations: dP/dt_{max}, the maximum rate of change in LV pressure; dP/dt_{min}, the minimum rate of change in pressure; HR, heart rate; LVDP, left ventricular developed pressure; n=3 per group.

A.
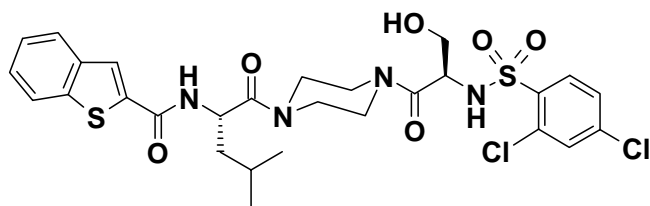
GSK1016790A
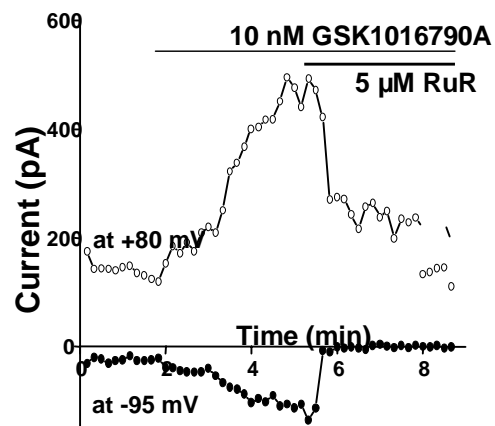
in vitro potencies

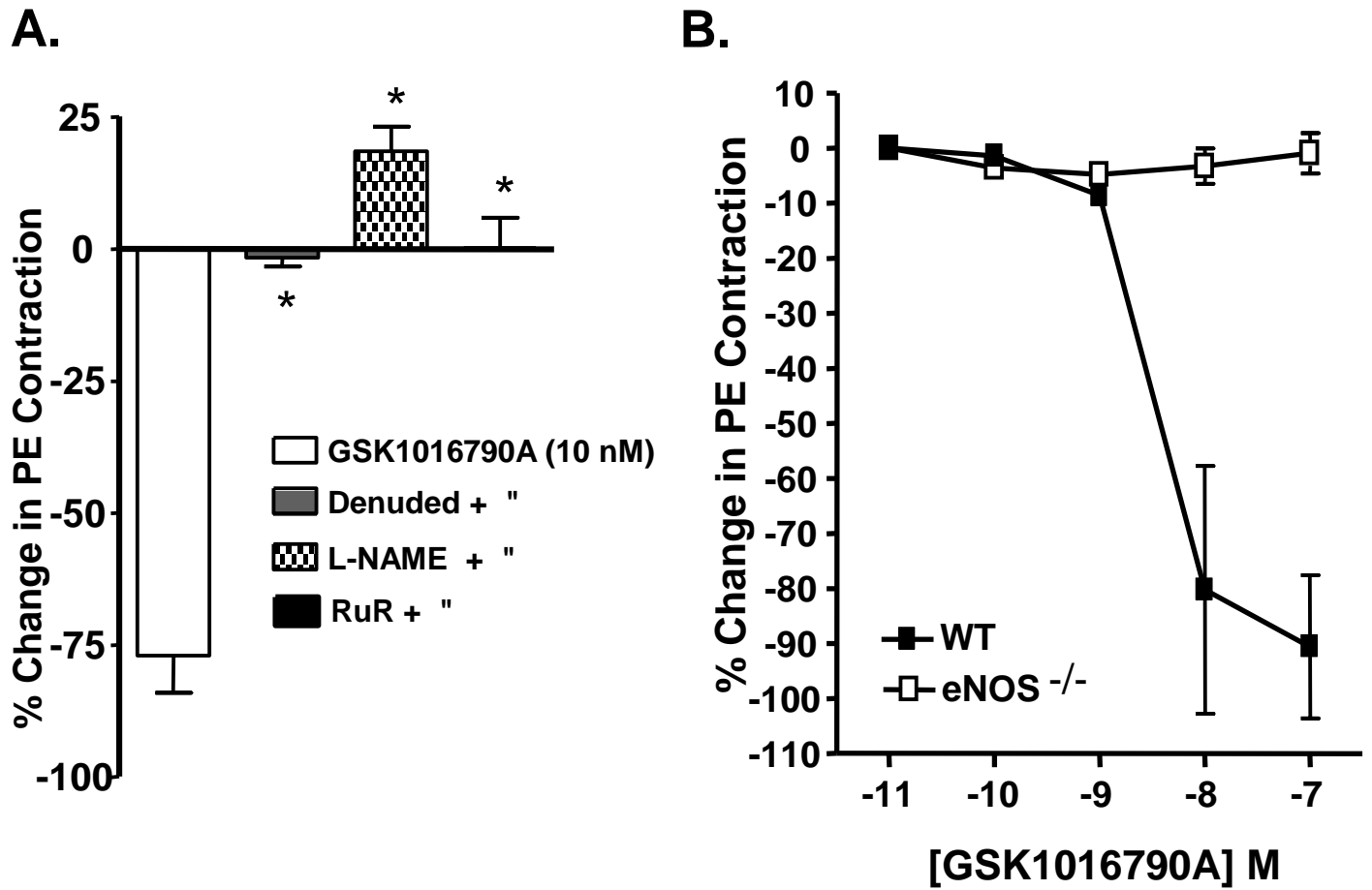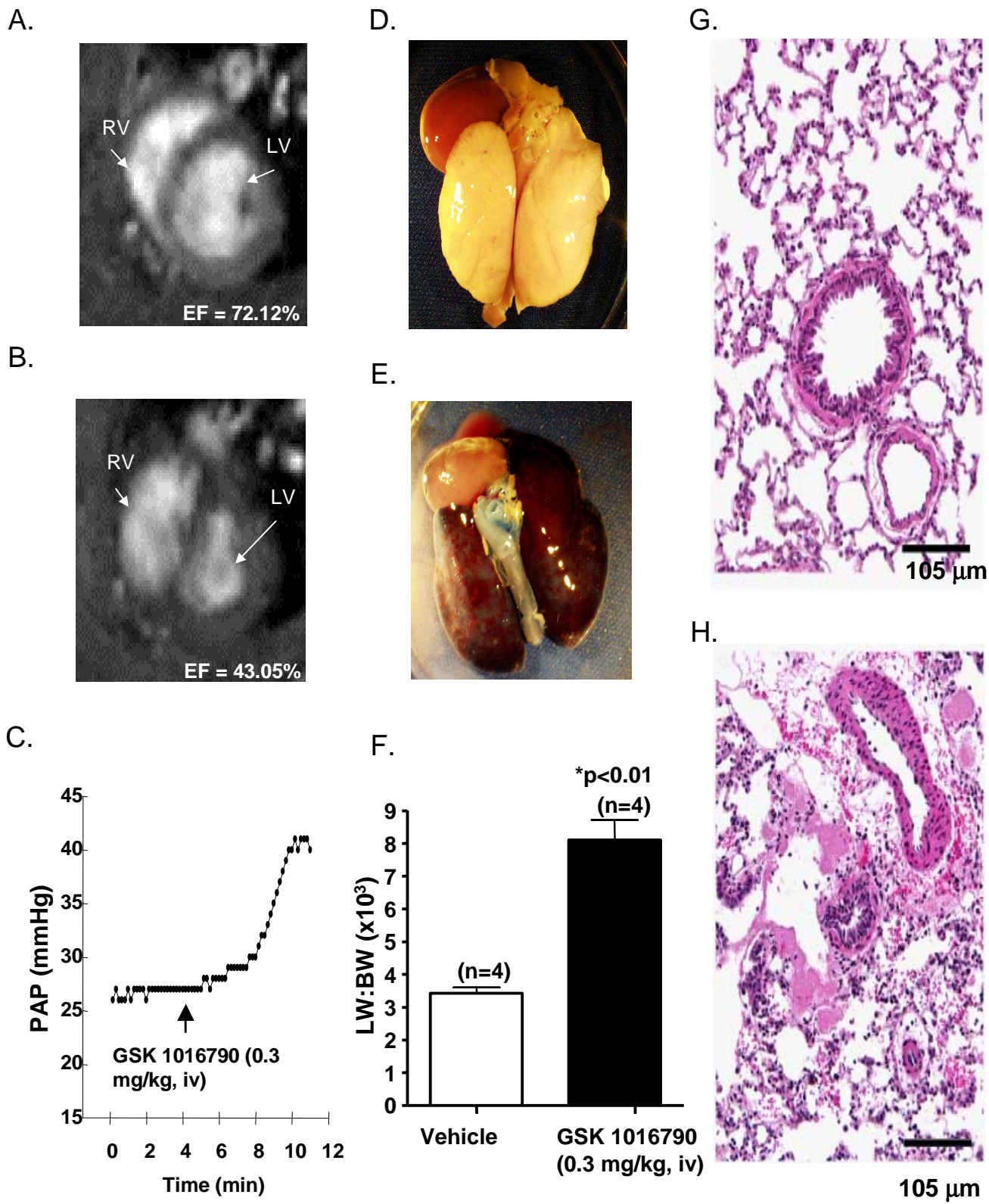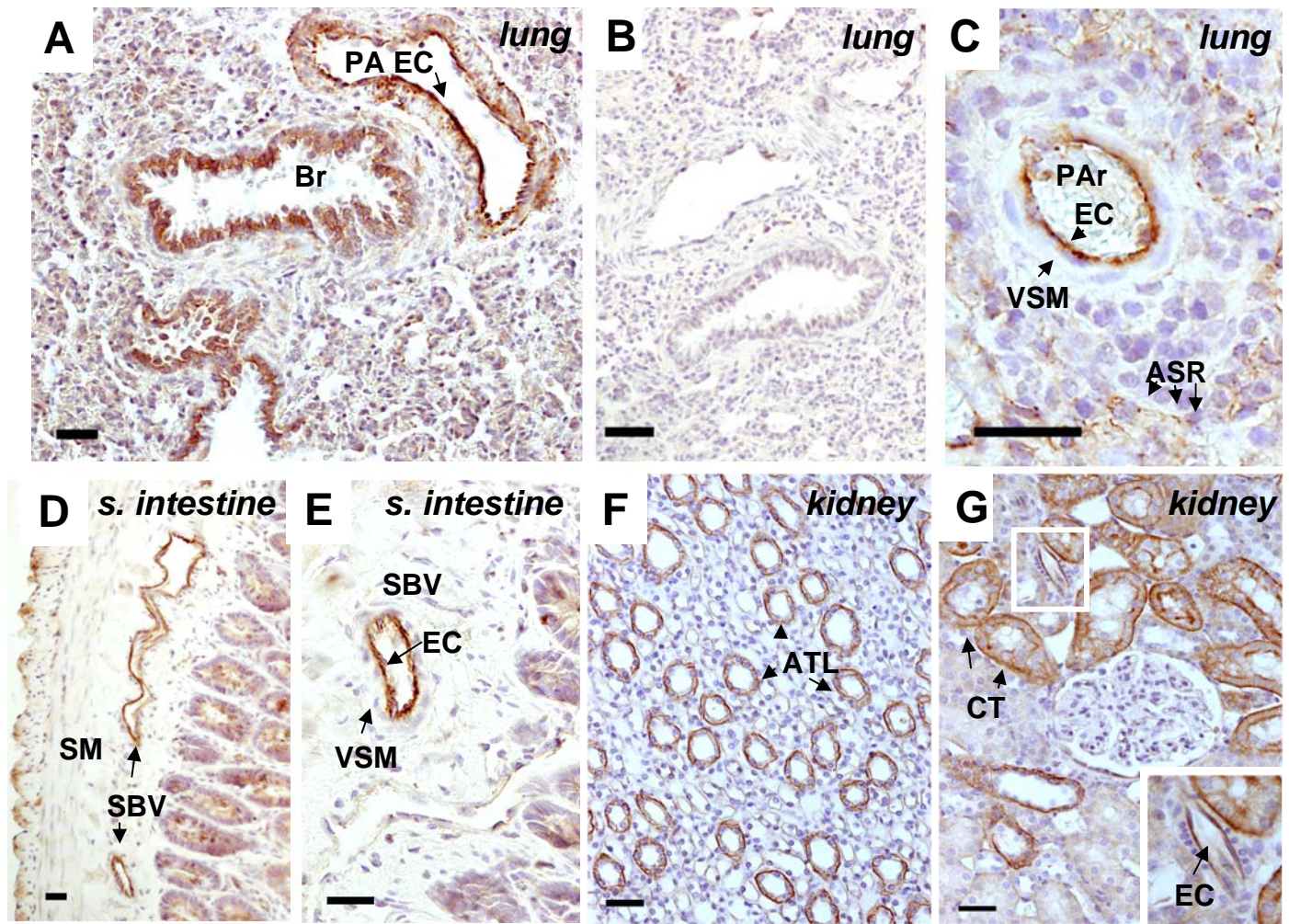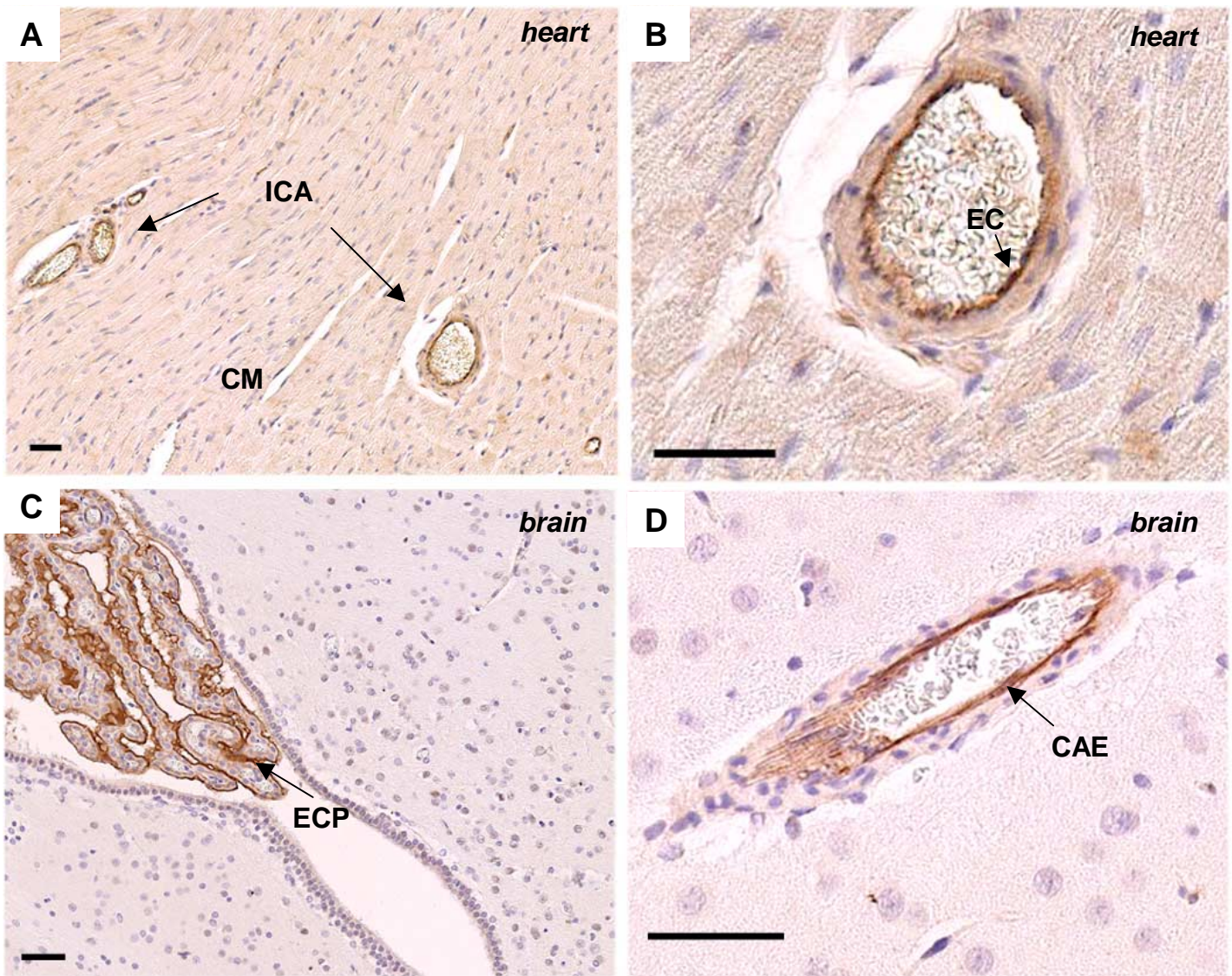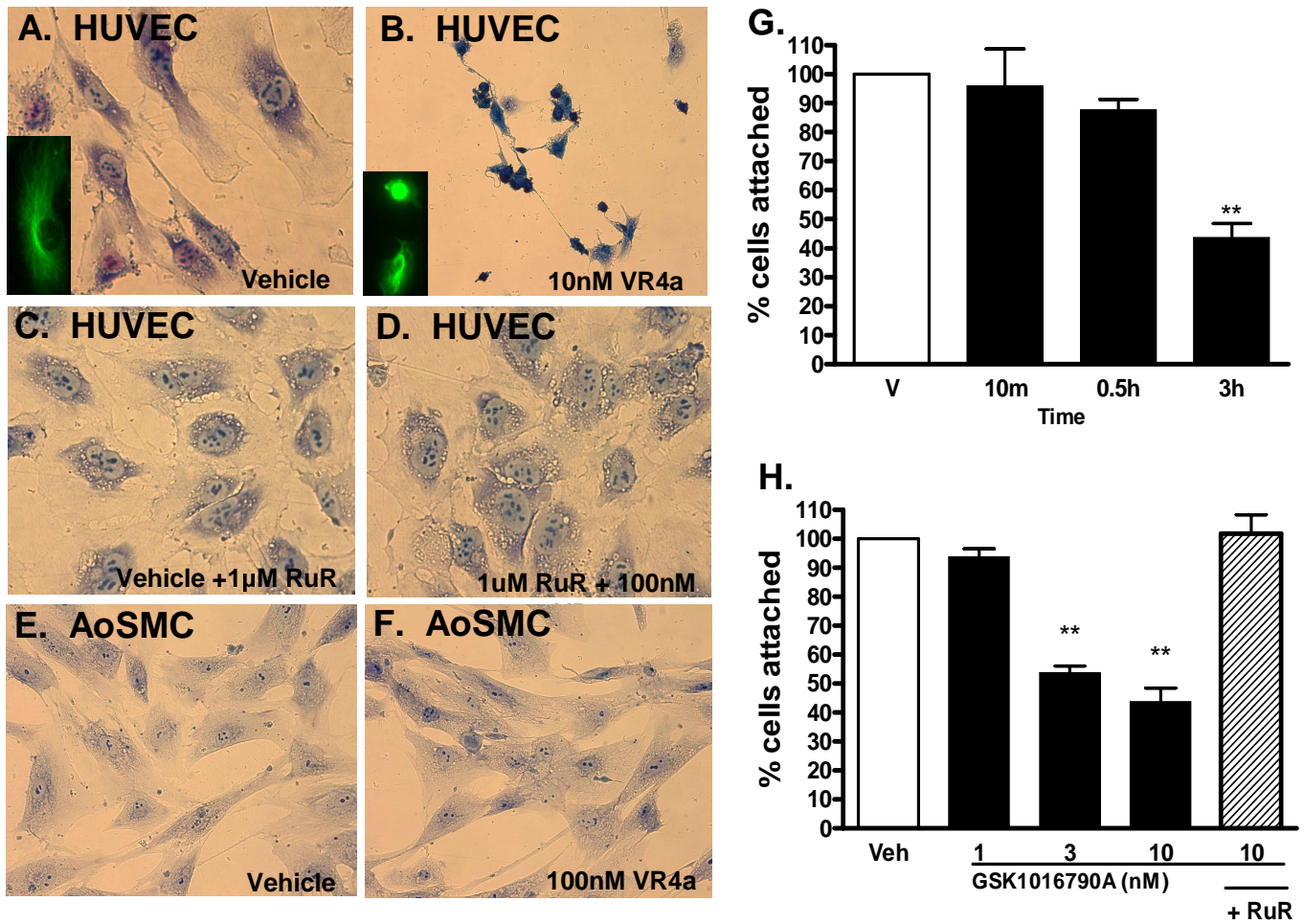| TRPV Assay	EC$_{50}$ (nM)
TRPV4 HEK FLIPR	5.0
Human Chondrocytes TRPV4	3.0
Bovine Chondrocytes TRPV4	1.0
Mouse Chondrocytes TRPV4	18.5
Rat Chondrocytes TRPV4	10
Dog Chondrocytes TRPV4	1.0
TRPV1 HEK FLIPR	50

B.
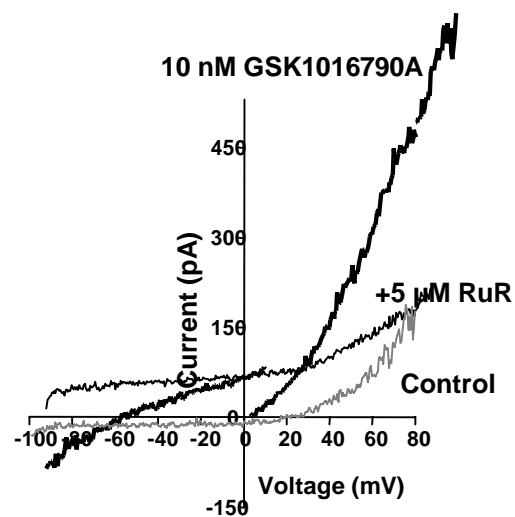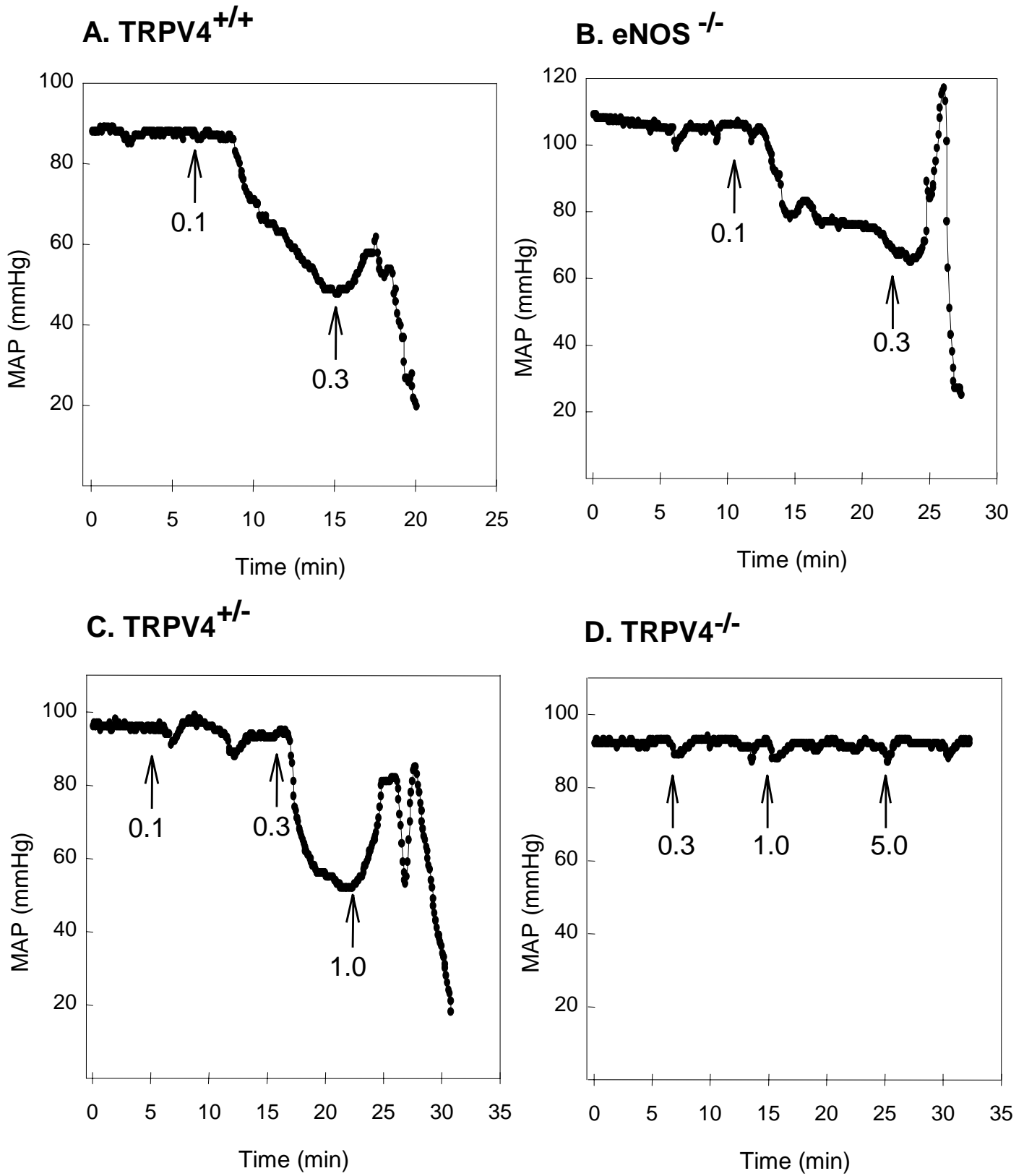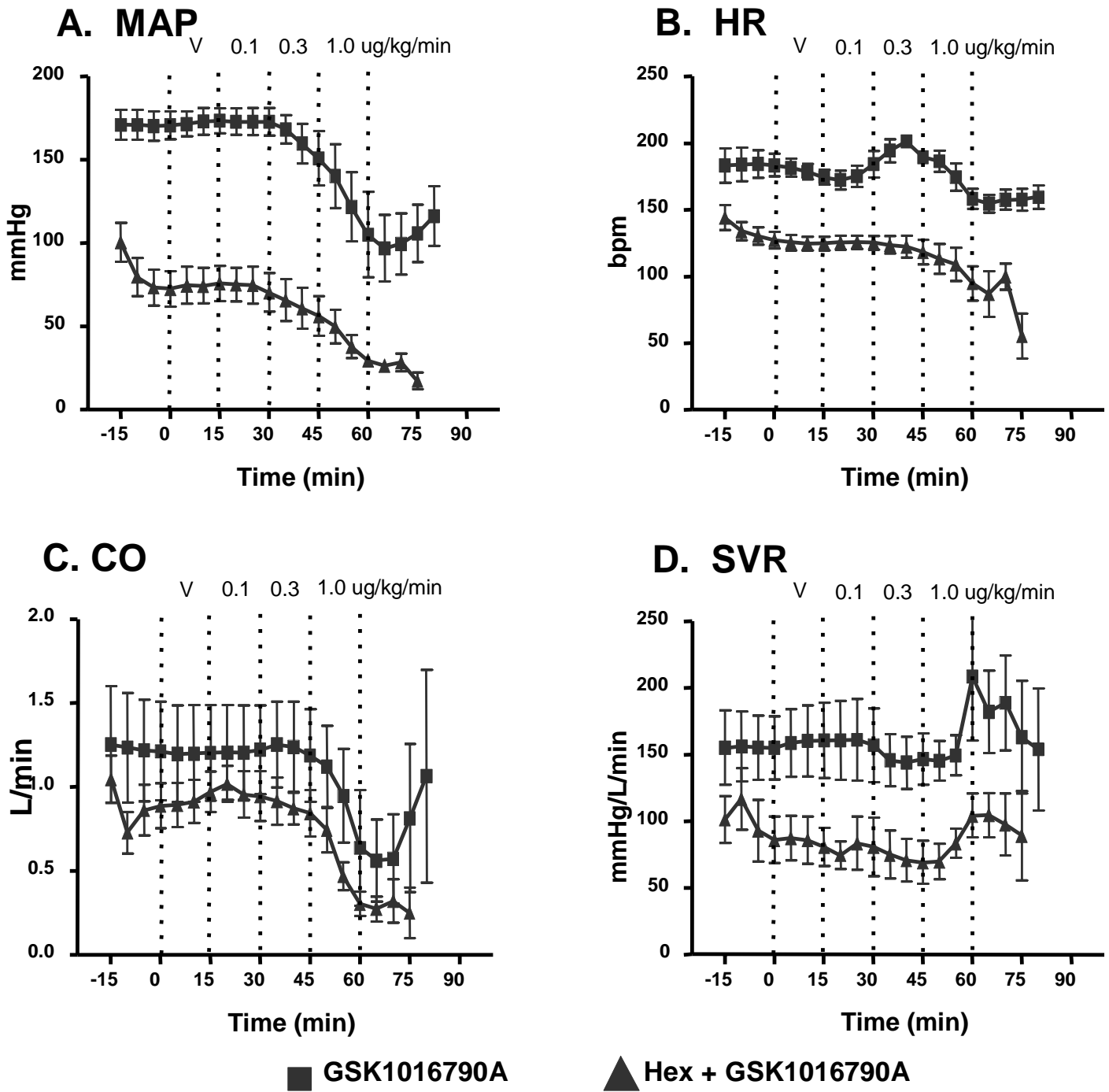
Figure 1

Figure 2

Figure 3

Figure 4:

Figure 5

Figure. 6

Figure. 7

Figure 8: